Earth and Planetary Science Letters 349–350 (2012) 153–160

Contents lists available at SciVerse ScienceDirect

Earth and Planetary Science Letters

journal homepage: www.elsevier.com/locate/epsl

The relationship of intermediate- and deep-focus seismicity to the hydration and dehydration of subducting slabs

C. Grace Barcheck [a,*], Douglas A. Wiens [a], Peter E. van Keken [b], Bradley R. Hacker [c]

[a] Department of Earth and Planetary Sciences, Washington University in St. Louis, Campus Box 1169, 1 Brookings Drive, St. Louis, MO 63130, USA
[b] Department of Earth and Environmental Sciences, University of Michigan, 2534 C. C. Little Building, 1100 North University Ave, Ann Arbor, MI 48109-1005, USA
[c] Department of Earth Science, University of California, 1006 Webb Hall – MC 9630, Santa Barbara, CA 93106-9630, USA

ARTICLE INFO

Article history:
Received 29 February 2012
Received in revised form
25 June 2012
Accepted 26 June 2012
Available online 9 August 2012

Keywords:
deep earthquakes
dehydration embrittlement
subduction zone
water

ABSTRACT

Previous studies suggest that intermediate- and deep-focus earthquakes in subducting slabs may result from dehydration reactions. We investigate the importance of dehydration in facilitating intermediate- and deep-focus earthquakes by comparing the seismicity rate with the calculated slab dehydration flux (van Keken et al., 2011) as a function of depth in 56 subduction zones worldwide. For each region, the seismicity rate per km of trench length per year as a function of depth between 1990 and 2009 was determined from the Preliminary Determination of Epicenters (PDE) catalog. The number of earthquakes between 75 and 240 km depth was compared to the calculated slab dehydration flux in 25 km increments. Deeper than 240 km, dehydration rates were not calculated, so seismicity is instead compared to the calculated flux of water that remains mineralogically bound in the slab at that depth. No strong correlation between the dehydration flux and the seismicity rate was found at any depth. This suggests that some factor besides the presence of water, such as the stress state of the slab, controls intermediate-focus seismicity. For depths greater than 240 km, there is a correlation between the amount of mineralogically-bound H_2O and the seismicity rate. In particular, although deep slabs with small amounts of bound water show a wide range of seismicity rates (and many have no seismicity whatsoever), all deep slabs with appreciable water transported below 240 km show significant seismicity. We conclude that the presence of water may be a necessary condition for deep seismicity in conjunction with other factors. We also note that slab temperature and dehydration are linked. Traditionally the limitations on deep earthquake occurrence have been linked to temperature, but this study suggests that similar arguments can be made linking deep earthquakes with the presence of water.

1. Introduction

Earthquakes generated by sudden brittle shear failure ought to be inhibited at depths greater than about 40–70 km where increased pressure and temperature favor ductile rather than brittle failure (Houston, 2007; Frohlich, 2006). Nevertheless, earthquakes have been observed to depths of nearly 700 km since the early days of seismology (Wadati, 1928). These "deep earthquakes" can be roughly separated into two populations based on their depth. Globally, deep earthquakes are characterized by an approximately exponentially decreasing number of events down to about 300 km depth, a minimum between 300 and 450 km depth, and another active zone between 450 and 680 km depth with a peak around 550–600 km (Houston, 2007; Frohlich, 2006). Here, we use the common convention to refer to earthquakes between 60 and 300 km depth as "intermediate-focus" events, and events deeper than 300 km as "deep-focus" events. "Deep earthquakes" refers to all events deeper than 60 km.

The exact mechanism of these earthquakes remains elusive, though several different possibilities have been proposed. Early workers suggested an implosive phase change could release seismic energy (e.g., Leith and Sharpe, 1936), but subsequent analysis has failed to find the large isotropic component expected in deep events caused by such a mechanism (e.g., Kawakatsu, 1991; Okal, 1996; Russakoff et al., 1997; Estabrook, 1999). Other suggested mechanisms include shear instabilities (Ogawa, 1987; Kelemen and Hirth, 2007), catastrophic plastic shear (Hobbs and Ord, 1988), transformational faulting and anticrack formation (e.g., Kirby, 1987; Green and Burnley, 1989; Green and Houston, 1995; Kirby et al., 1996), and dehydration embrittlement (e.g., Hubbert and Rubey, 1959; Griggs and Handin, 1960; Raleigh and Paterson, 1965; Green

* Corresponding author. Tel.: +1 314 941 2652.
E-mail address: barcheck@seismo.wustl.edu (C.G. Barcheck).

and Houston, 1995; Dobson et al., 2002; Hacker et al., 2003; Jung et al., 2004). It is important to note that 'dehydration embrittlement' sensu stricto refers to the embrittlement of rock actively dehydrating, whereas 'hydration embrittlement' is a better term for embrittlement produced by the presence of fluid produced at any distance from the fault and at any time. The former has only been demonstrated in experiments (e.g., Lee and Kirby, 1984)—and requires special circumstances to operate—whereas the latter is a central tenet of rock mechanics at all scales (e.g., Scholz, 1989).

The presence of subducted water is crucial for several proposed mechanisms of intermediate and/or deep seismicity. The dehydration embrittlement mechanism suggests that as subducted material sinks into the mantle and is subjected to higher temperature and pressure, hydrated crustal and mantle minerals dehydrate. Theoretically, this fluid increases pore pressure, reduces normal stress and friction across a potential fault, and facilitates brittle fracture and slip. Subducted water may also play a role in mechanisms in which lenses of ultra-fine-grained byproducts of dehydration reactions form in subducting rocks, enabling faulting (Frohlich, 2006). Zhang et al. (2004) proposed another mechanism in which hydroxyl defects in eclogite precipitate at grain boundaries, producing small amounts of melt and creating another dehydration-related faulting instability. They suggested that this mechanism could be important in the transition zone (400–700 km depth), where earthquakes occur despite all major hydrous phases likely having decomposed in the upper mantle (Green et al., 2010).

There is significant evidence from thermal–petrologic models, fieldwork, and laboratory work that dehydration embrittlement is the probable mechanism for intermediate-focus events. Several workers have found the locations of earthquakes to correspond well with predicted dehydration loci in downgoing slabs, suggesting that intermediate-focus earthquakes are caused or facilitated by dehydration reactions (Hacker et al., 2003; Yamasaki and Seno, 2003; Mishra and Zhao, 2004). These models, which are based on thermal and petrological modeling (Yamasaki and Seno, 2003; Hacker et al., 2003) and P-wave velocity structure models (Mishra and Zhao, 2004) extend only to the upper few hundred km of the modeled subduction zones, leaving the deeper parts of subducted slabs less understood.

Evidence of dehydration embrittlement is abundant in naturally deformed rocks (e.g., Healy et al., 2009), and has been reported in a wide variety of experimentally deformed materials (e.g., Raleigh and Paterson, 1965; Murrell and Ismail, 1976; Lee and Kirby, 1984; Dobson et al., 2002; Jung et al., 2004; Chollet et al., 2009). Whether similar mechanisms operate in Earth's transition zone remains unclear, given the difficulty of reproducing those conditions in the lab and the improbability of finding rocks from extreme depths exhumed to the surface.

If dehydration reactions are the primary mechanism for producing intermediate and/or deep earthquakes, we should expect to see some relationship between seismicity and the amount of water subducted to various depths. At a minimum, dehydration reactions require the presence of water, and subducting slabs at temperatures and pressures greater than the dehydration conditions should be anhydrous and thus aseismic if dehydration embrittlement is operative. We may also expect to find a correlation between modeled dehydration fluxes and the seismicity rate, if the seismicity mechanism is sensitive to the amount and distribution of water in the slab. This paper investigates the relationship between subducted water and seismicity rates by comparing the locations and depths of earthquakes in the global catalog to results from the dehydration models of van Keken et al. (2011) for 56 subduction zones worldwide. The results provide some constraints on the possible role of water in producing intermediate and deep seismicity.

2. Methods

2.1. Slab dehydration calculations

Van Keken et al. (2011), hereafter referred to as "vK11" produced models of the metamorphic facies and H_2O content of 56 subducting slabs worldwide using the "D80" thermal models of Syracuse et al. (2010). These models use updated subduction-zone geometries based on Syracuse and Abers (2006) and represent nearly all active trenches worldwide (see Fig. 1). The relevant equations are solved on a high-resolution, finite-element mesh to produce petrological models of subducting slabs and calculations of the dehydration flux at various depths down to 240 km. Slab crust is modeled following Hacker (2008), with a variable-thickness sediment layer, a 300 m thick upper volcanic layer, a 300 m thick lower volcanic layer, 1.4 km of dikes, and 5 km of gabbro. Because the hydration state of the upper mantle is poorly constrained, vK11 produced three models with different hydration assumptions for the upper 2 km of the mantle: dry, 2 wt% H_2O, and fully hydrated. Subsolidus phase relations in the slab and overlying mantle wedge were calculated using Perple_X (Connolly, 2009), the 2004 version of the Holland and Powell (1998) thermodynamic database, and Syracuse et al. (2010) "D80" thermal models. Hypersolidus phase relations for crustal rocks were determined from the experimental literature, primarily from Schmidt et al. (2004).

We use vK11's moderate upper mantle hydration case—2 wt% H_2O in the upper 2 km of the mantle—as a conservative model of upper mantle hydration (Model 1). A less conservative model is motivated by seismic results from Van Avendonk et al. (2011), who used mantle V_p velocities from the subducting Cocos plate off Nicaragua to estimate ~3.5 wt% bound H_2O. This model (Model 2) has 4 wt% H_2O in the upper 4 km of the mantle and 2 wt% H_2O to 8 km depth. We compare the calculated dehydration fluxes in Model 1 and Model 2 with actual slab seismicity between 1 January 1990 and 31 March 2009 to assess whether there is a relationship between seismicity and dehydration.

2.2. Seismicity rate determination

We determine appropriate analysis volumes for each of vK11's 56 trench locations based on the extent of the adjacent seismically active area, the azimuth of slab subduction, and proximity to the next datum. If nearby data are unavailable, the end of the trench or the edge of the seismically active area determines the edges of the analysis volume. The seismically active area is determined by visually examining earthquake event data in map view. Earthquakes inside these analysis volumes are considered to be related to the slab mineralogy and other slab parameters at the data point.

We use the surface coordinates of the corners of these volumes to query two databases, the Preliminary Determination of Epicenters (PDE) database and the Centroid Moment Tensor (CMT) catalogue, between 1 January 1990 and 31 March 2009. The PDE database provides data on the number of earthquakes above a chosen body wave magnitude threshold at predetermined depths within each analysis volume, and the CMT catalogue provides data on the sum of the seismic moments of all earthquakes at those same predetermined depths. We select a body-wave magnitude threshold of $m_b \geq 4.5$, as the catalog is relatively complete at this magnitude level for most slabs. We do not remove aftershocks from our data because aftershock sequences that can be recorded globally are rare following intermediate- or deep-focus earthquakes (Frohlich, 2006). We gather the data from the PDE and the CMT into bins in 25 km increments between 75 and 240 km depth for comparison with the corresponding vK11 model

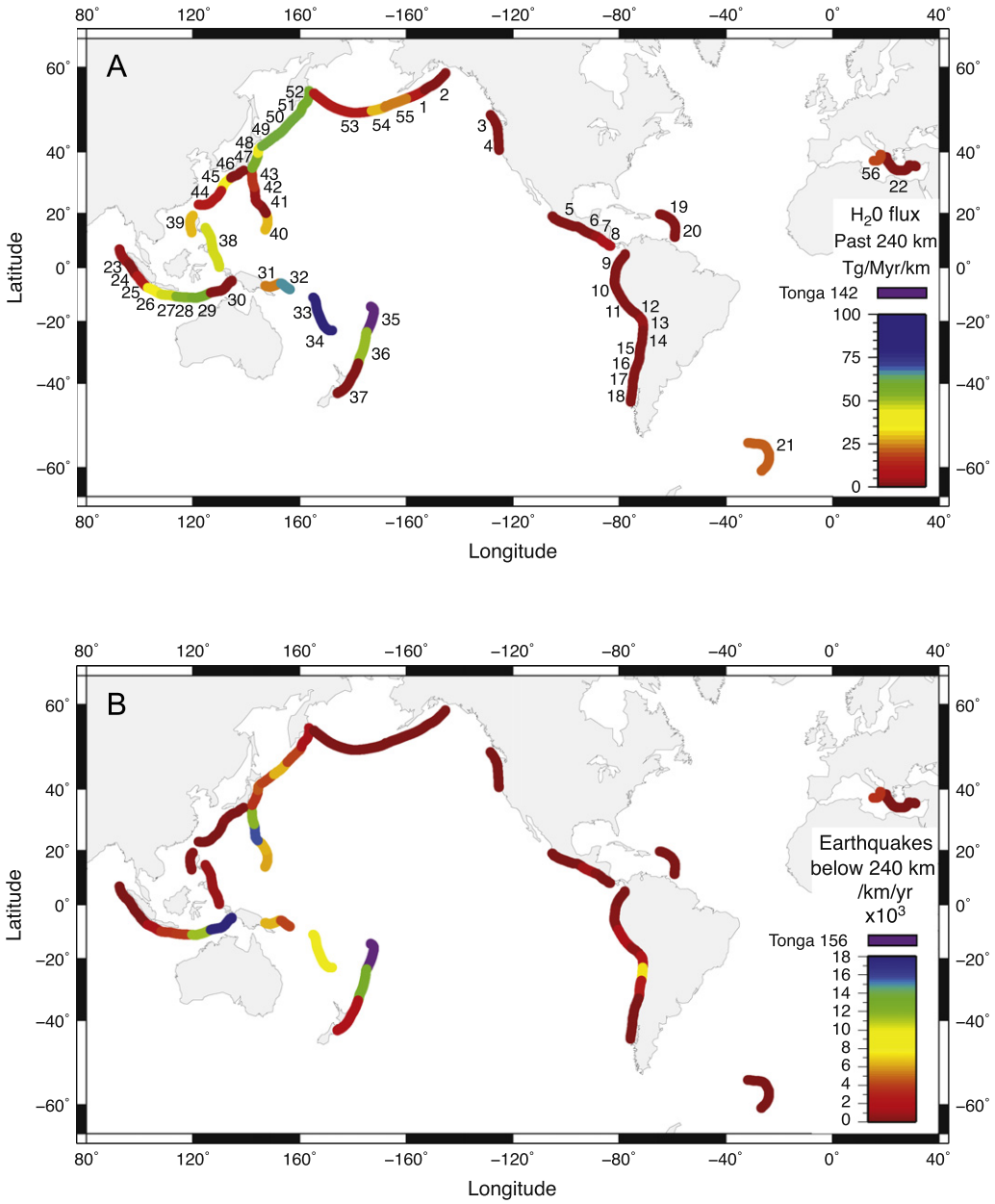

Fig. 1. World location maps showing (A) amount of H_2O held mineralogically past 240 km depth calculated from vK11's Model 2 for each subduction zone, and (B) number of earthquakes per km along trench per year calculated from the PDE for each subduction zone analysis volume. Subduction zone labels in (A) correspond to the values in Table 1 and to the numbering scheme used in vK11. Note that for Tonga, denoted here by purple, H_2O flux is considerably higher than in any other subduction zone, and seismicity is a full order of magnitude greater.

results summed over those same depths. All data are normalized by the along-trench width of the analysis volume to correct for variation in analysis volume size and by the number of years in our sample. It is useful to note that the moment sums are much less robust than the seismicity rates, because they are controlled by the one or two largest earthquakes in the region and are thus more subject to uncertainty resulting from the limited observation time. Our observation period of 20 yr is too short relative to the recurrence interval of the largest events to include the largest events possible in all subduction zones in our sample. This creates a bias toward zones with recent large earthquakes. We consequently direct our analysis to the seismicity rate data.

Because vK11 did not calculate H_2O dehydration fluxes deeper than 240 km due to increasing uncertainty in phase relations below that depth, deeper seismicity data are instead compared to the amount of crystal-bound H_2O subducted past 240 km in each model. Thus, earthquakes occurring below 240 km depth cannot be correlated directly with predicted dehydration loci, but rather with the possibility that crystal-bound H_2O may be present and may participate in causing seismicity. This quantity, H_2O subducted past 240 km, was compared to seismicity over three depth intervals: 240–400 km, 400–700 km, and 240–700 km. These depth intervals correspond to the two global populations of earthquakes occurring between ~70 and ~300 km depth in the upper mantle and ~400 km and deeper in the transition zone (Frohlich, 2006), in addition to all deep-focus earthquakes globally. Relating earthquake data integrated over hundreds of km to the amount of water subducted past 240 km depth is a coarse

comparison, necessitated by uncertainties in the phase diagrams of hydrous materials below 240 km depth. Nevertheless, this comparison may hold important insights.

Our analysis volumes are designed to select the population of seismic events most related to the present-day subduction parameters used in vK11. We consider the current geometry of each subduction zone and our analysis volumes are therefore chosen along the present-day azimuth of slab convergence (from Syracuse et al., 2010), which we note is not always an accurate reflection of slab convergence in the past. For a small number of slabs, the azimuth of convergence is extremely oblique to the trench normal, and it is highly uncertain whether we are associating the correct population of deep events with vK11's dehydration calculations. Because of this uncertainty, we removed from our figures all data from zones in which the present-day azimuth of slab subduction differs from trench-normal by more than 55°. Consequently, data from the New Britain, North Marianas, North Philippines, and East Banda Sea subduction zones are not shown in our figures. Nor are seismicity rates calculated at the Nankai subduction zone, which overlies deep earthquakes occurring along the contours of the Pacific plate subducting at the Japan and Izu–Bonin trenches. These deep events are best associated with the Izu or Central Honshu subduction zones, and it is unclear which, if any, events should be associated with Nankai.

3. Results

At the intermediate depths corresponding to vK11's models (75–240 km depth), we find no correlation between the H_2O dehydration flux predicted by either model and seismicity at any depth (Fig. 2). The data instead exhibit no identifiable pattern: there are subduction zones with a large H_2O flux and little seismicity, and vice versa. This result is somewhat surprising, because of the argument that intermediate-focus earthquakes are caused or facilitated by dehydration reactions (e.g., Green and Houston, 1995; Hacker et al., 2003; Yamasaki and Seno, 2003; Kita et al., 2006). We also do not find a correlation between the seismic moment sum and dehydration flux in any intermediate depth range.

At depths below vK11's calculations (240–700 km depth), we find only a small correlation between the amount of H_2O carried deeper than 240 km in either model and seismicity below that depth (Fig. 3, Table 1). We do observe, however, a stronger relationship between the H_2O flux past 240 km depth and the median number of earthquakes per km along trench per year in zones with similar H_2O fluxes (Fig. 3, grey bars). Between 240 and 700 km deep, all zones with a calculated H_2O flux past 240 km of $> \sim 5$ Tg/Myr/km in Model 1 (Fig. 3C), and $> \sim 10$ Tg/Myr/km in Model 2 (Fig. 3F) show at least some seismicity, and in both models the median number of events per km per year increases with H_2O flux past 240 km depth. This suggests that the minimum number of events depends in some way on hydration of the deep slab, with greater hydration in general facilitating more earthquakes, though not in a regular, identifiable way. We find no correlation between the seismic moment sum and the amount of H_2O past 240 km depth, but, as noted earlier, the moment sums depend on only one or two large earthquakes in each region.

4. Discussion

The observed lack of correlation between dehydration flux and seismicity at intermediate depths (75–240 km depth, Fig. 2) is notable because many workers have suggested that

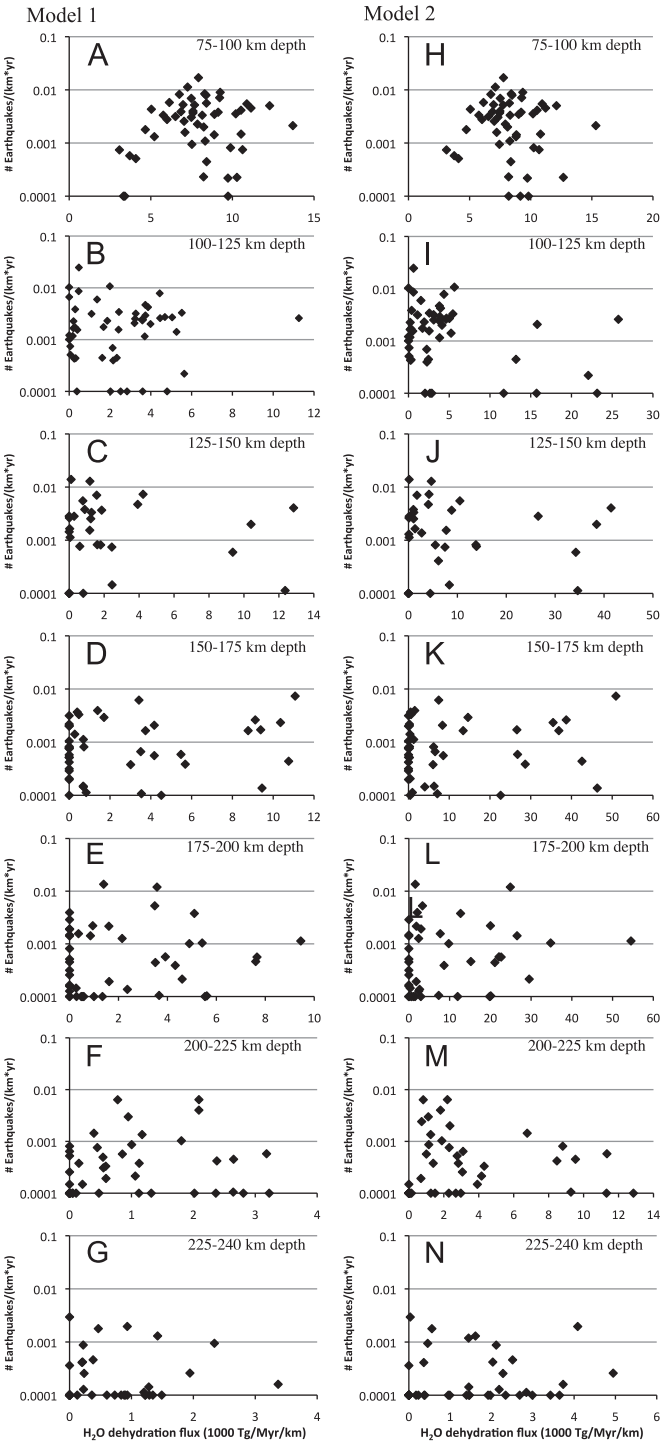

Fig. 2. Earthquakes per km along trench per year as a function of dehydration flux, in 25 km depth increments. (A–G) are Model 1 results, calculated using an estimate of upper mantle hydration of 2 wt% H_2O in the upper 2 km of the mantle. (H–N) are Model 2 results, calculated using the less conservative estimate of 4 wt% H_2O in the upper 4 km of the mantle, and 2 wt% H_2O to 8 km mantle depth. Model 2 is based on the results of Van Avendonk et al. (2011), who used mantle V_p velocities to find 3.5 wt% H_2O in the upper mantle beneath the subducting Cocos plate. The number of earthquakes from the Preliminary Determination of Epicenters (PDE) with $m_b \geq 4.5$ in each depth range is divided by the along trench width of the analysis volume and the number of years sampled. These values are plotted against the net H_2O released in each depth increment, summed from vK11's model results. Figures are plotted with a logarithmic y-axis to better display results from zones with small numbers of earthquakes. These results show no correlation between seismicity rate and dehydration flux in this depth range.

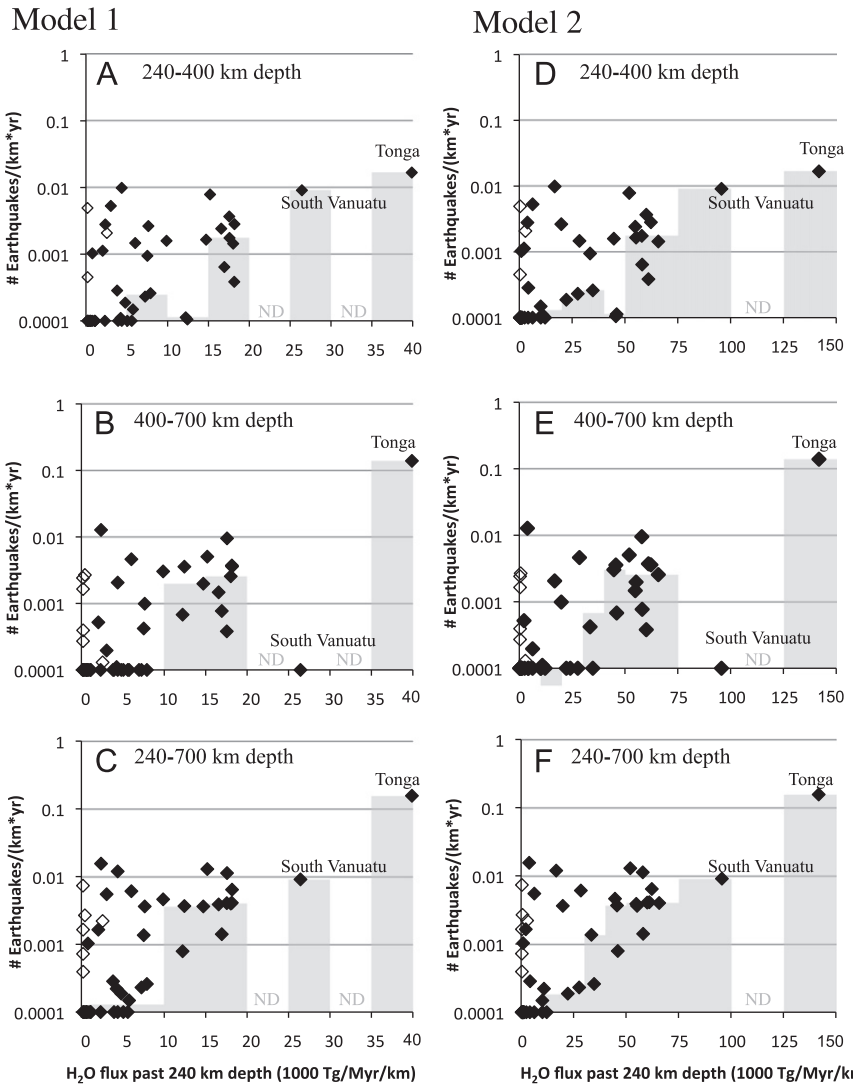

Fig. 3. Intermediate- and deep-focus results, in depth ranges of 240 to 400 km depth, 400 to 700 km depth, and integrated between 240 and 700 km depth. (A–C) are Model 1 results (2 wt% H_2O in the upper 2 km of the mantle). (D–F) are Model 2 results (4 wt% H_2O in the upper 4 km of the mantle, 2 wt% H_2O to 8 km). Diamonds indicate the number of earthquakes per km along trench per year in each analysis volume plotted against the amount of H_2O retained mineralogically in the slab past 240 km depth, which is the deepest that the dehydration flux is calculated in vK11's models. Open diamonds indicate South American subduction zones (Peru through South Central Chile) that likely retain more water past 240 km depth than in vK11's model. Grey bars represent the median number of events per km along trench in each subduction zone binned by H_2O flux past 240 km depth. Model 1 results are binned in increments of 5×10^3 Tg/Myr/km. Model 2 results are binned in increments of 10×10^3 Tg/Myr/km up to 50×10^3 Tg/Myr/km, and 25×10^3 Tg/Myr/km thereafter. ND indicates no median data; blank columns are zero values. We observe an increasing minimum number of earthquakes per km per year with increasing H_2O flux past 240 km between 240 and 700 km depth (C,F). Generally, subduction zones with higher H_2O fluxes past 240 km depth also have higher median numbers of earthquakes per km per year at all depths below 240 km. Tonga and South Vanuatu are labeled; Tonga has by far the largest amount of subducted water due to the fast subduction of old oceanic lithosphere. The South Vanuatu subduction zone formed recently, and thus it is unclear whether the slab has yet penetrated to depths greater than 400 km, possibly explaining the lack of deep-focus seismicity (e.g., Hamburger and Isacks, 1987).

intermediate-focus events are related to dehydration embrittlement (e.g., Green and Houston; 1995, Hacker et al., 2003; Yamasaki and Seno, 2003). Our observations suggest four possibilities to explain the lack of correlation. First, slab input parameters and local geometry variations may not be known well enough for vK11's resulting model to accurately reflect actual dehydration rates in all cases. Thus, any relationship between dehydration and seismicity may be obscured because of the limitations of the dehydration model. Second, dehydration reactions may not cause or facilitate intermediate-focus events at all; some entirely different mechanism is at work. Third, other factors such as slab stress or strain rate may also participate in determining the rate of intermediate-focus seismicity. For example, two identical slabs with different stress states may exhibit different amounts of seismicity despite having the same dehydration flux. Or, finally, intermediate-focus events may be caused by the hydrous products of dehydration rather than the dehydration reaction itself. If those products facilitate seismicity only under certain conditions, the events could occur at some distance in space and time from this initial zone of dehydration. In this case, there would be no clear relationship between dehydration and seismicity, similar to what we observe. Our results suggest that dehydration embrittlement cannot be the primary factor controlling the occurrence of intermediate-focus earthquakes.

Deeper than 240 km, our results are more intriguing. Fig. 3A–F show a lot of scatter, similar to our shallower results. However, Fig. 3C and F do show a relationship between H_2O flux past 240 km depth and a minimum amount of seismicity. Between 240 and 700 km depth, all zones with an H_2O flux past 240 km of $> \sim 5$ Tg/Myr/km (Model 1) or $> \sim 10$ Tg/Myr/km (Model 2) have some earthquakes (Fig. 3C and F), and in general the minimum number of events increases with H_2O flux past 240 km.

Table 1

	Subduction zone	H_2O subducted past 240 km depth		Seismicity rate		Thermal parameter (Φ)
		Model 1 (1000 Tg/Myr/Km)	Model 2 (1000 Tg/Myr/Km)	240–400 km depth (# earthquakes/(km × yr) × 10^3)	400–700 km depth (# earthquakes/(km × yr) × 10^3)	(km)
1	Alaska Peninsula	5.06	10.16	0	0	2200
2	Alaska	1.12	1.23	0	0	1560
3	British Columbia	0.79	0.91	0	0	130
4	Cascadia	0.59	0.68	0	0	100
5	Mexico	0.59	0.71	0	0	400
6	Guatemala-El Salvador	0.78	0.96	1.03	0	970
7	Nicaragua	3.82	4.28	0.28	0	1100
8	Costa Rica	5.60	6.27	0	0	1010
9	Columbia Ecuador	0.16	0.32	0.07	0	420
10	N Peru[a]	0.21	0.39	0	0.39	360
11	C Peru[a]	0.20	0.38	0	1.65	520
12	Peru[a]	0.20	0.37	0.45	0.27	1340
13	N Chile[a]	2.56	2.88	2.08	0.13	1780
14	NC Chile[a]	0.19	0.38	4.93	2.41	1330
15	C Chile 1[a]	0.42	0.66	0	2.68	660
16	C Chile 2[a]	1.05	1.28	0	0	1070
17	SC Chile[a]	1.10	1.34	0	0	860
18	S Chile	0.27	0.48	0	0	430
19	N Antilles	0.19	0.23	0	0	1110
20	S Antilles	0.35	0.40	0	0	1040
21	Scotia	4.82	22.25	0.19	0	2860
22	Aegean	0.57	0.61	0	0	1520
23	N Sumatra	3.93	4.17	0	0	1510
24	C Sumatra	2.32	2.49	0	0	1590
25	S Sumatra	4.25	10.90	0.11	0.11	2590
26	Sunda Strait	7.52	33.51	0.94	0.42	3960
27	Java	12.43	45.71	0.10	3.57	5400
28	Bali-Lombok	16.56	54.89	2.41	1.47	6770
29	W Banda Sea	17.58	57.99	1.75	9.51	5980
30	E Banda Sea[b]	0.23	0.29	17.16	2.68	1950
31	New Britain[b]	12.23	24.59	2.67	3.71	2310
32	Solomon	18.03	65.80	1.44	2.56	2710
33	N Vanuatu	3.05	6.29	5.29	0.20	1940
34	S Vanuatu	26.44	95.70	9.09	0	5180
35	Tonga	39.89	141.83	16.77	139.18	14320
36	Kermadec	15.19	52.03	7.87	5.05	5660
37	New Zealand	2.04	2.23	1.13	0.52	2420
38	S Philippines	12.21	46.08	0.11	0.68	3630
39	N Philippines[b]	9.10	28.90	0.26	0	2360
40	S Marianas	6.03	28.48	1.47	4.62	6350
41	N Marianas[b]	0.12	0.16	6.38	0	1990
42	Bonin	2.37	3.84	2.79	12.74	4080
43	Izu	4.38	16.73	9.88	2.06	4410
44	Kyushu	7.91	34.79	0.26	0	1560
45	Ryukyu	5.75	10.13	0.15	0	1710
46	Nankai[c]	0.54	0.65	ND	ND	450
47	C Honshu	14.71	55.28	1.65	1.98	6040
48	N Honshu	9.87	44.75	1.59	3.03	5070
49	Hokkaido	17.55	60.10	3.67	0.38	5720
50	S Kurile	18.18	62.30	2.82	3.59	6070
51	N Kurile	18.16	61.12	0.38	3.72	6360
52	Kamchatka	16.94	58.16	0.64	0.77	5410
53	W Aleutians	4.38	12.20	0	0	2350
54	C Aleutians	7.25	27.68	0.23	0	2840
55	E Aleutians	6.95	24.14	0.10	0	2540
56	Calabria	7.64	19.87	2.64	0.99	5830

Seismicity rates are all earthquakes in each analysis volume with $m_b \geq 4.5$.
Thermal parameter values are from Syracuse et al. (2010).

[a] Indicates South American slabs that likely retain more H_2O below 240 km than in vK11's models because the subducting Nazca plate was older, colder, and faster-moving when subducted 10–20 Ma (from the reconstructions of Sdrolias and Muller, 2006).

[b] Indicates extremely oblique subduction zones, not shown in Fig. 2–4.

[c] The Nankai data point in vK11 overlies earthquakes occurring along the Pacific Plate subducting at the Izu-Bonin and Japan trenches. These earthquakes are not associated with subduction of the Phillipine Sea plate at the Nankai trench, so no data from Nankai are included.

This suggests that H_2O plays some role in facilitating deeper seismicity, but the total number of events depends on some other factor. In support of this idea, Fig. 3A–F show that, in general, subduction zones with a greater H_2O flux past 240 km depth tend to have more earthquakes. The trend is stronger in Model 2, but it is evident in both models.

Fig. 3 suggests that H_2O plays a role in seismicity beneath 240 km, and that slabs containing significant water cannot be completely aseismic. Whether the actual mechanism is dehydration embrittlement or whether H_2O facilitates some other rupture mechanism is unclear. Below the 410 km discontinuity, the mechanism may not be the same embrittlement mechanism as

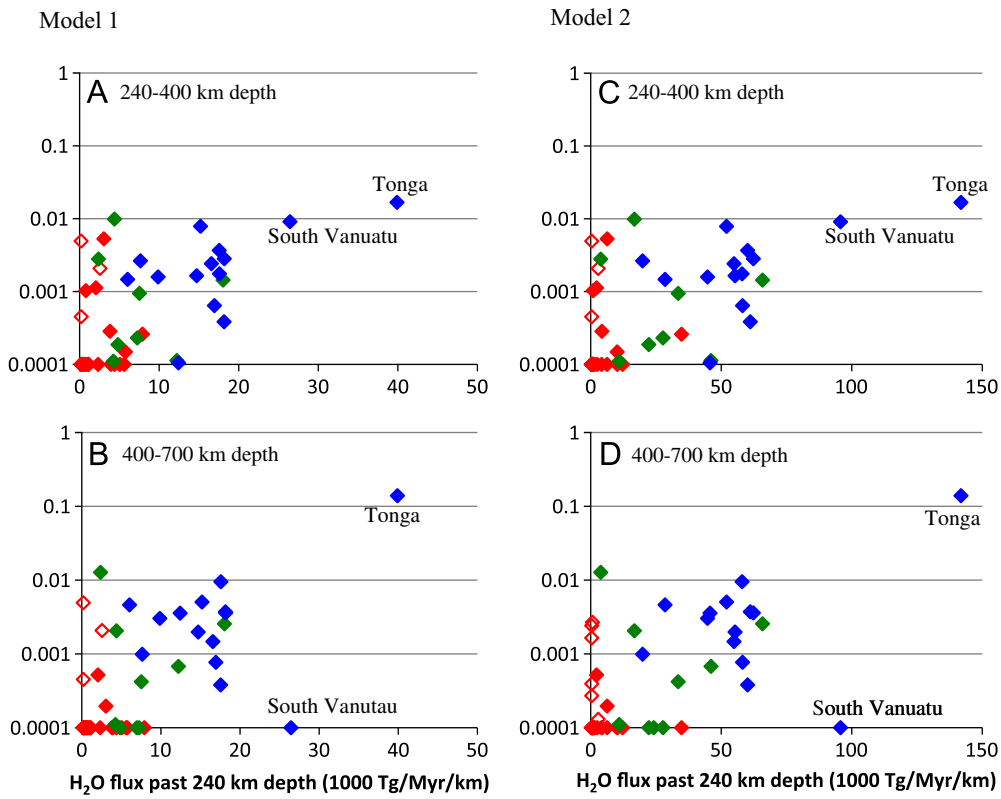

Fig. 4. Temperature dependence of dehydration reactions. Data between 240 and 700 km depth are colored by thermal parameter (Φ) from Syracuse et al. (2010). Hot slabs (2500 > Φ) are red, intermediate temperature slabs (5000 km > Φ > 2500 km) are green, and cold slabs (Φ > 5000 km) are blue. (A–B) are Model 1 results (2 wt% H_2O in the upper 2 km of the mantle). (C–D) are Model 2 results (4 wt% H_2O in the upper 4 km of the mantle, 2 wt% H_2O to 8 km). South American slabs are indicated with open diamonds. The hot slabs are clustered near each other, the cold slabs are clustered near each other, and the intermediate temperature slabs lie in between. (For interpretation of the references to colour in this figure legend, the reader is referred to the web version of this article.)

at shallower depths. Nevertheless, deep seismicity appears to be somewhat correlated with the presence of H_2O or its capacity to facilitate rupture via an unidentified mechanism, with the total number of events depending on some other factor.

If deep-focus seismicity is caused entirely by dehydration reactions, slabs should exhibit no seismicity below the depth of full dehydration. However, Fig. 3 illustrates that several slabs have a zero or near-zero calculated H_2O flux past 240 km, yet still exhibit relatively high seismicity. Several of these slabs, from North Peru through South-Central Chile, are all subduction zones where the Nazca plate is descending beneath South America. Recent relative plate-motion reconstructions show that plate-motion rates have slowed and the age of the subducting lithosphere has decreased considerably over the past 10–20 Myr (Sdrolias and Müller, 2006; Capitanio et al., 2011). Because lithosphere now at depths of ~300 km beneath South America would have subducted at roughly 10 Myr, and lithosphere at 600 km depth subducted at 20 Myr, the present-day subduction parameters used in vK11 may not be appropriate for lithosphere now at these depths. Older lithosphere subducting faster at 10–20 Myr would result in a colder slab than in vK11's model and allow more water to be subducted past 240 km depth. In this scenario, the South American subduction zones are not deep seismic zones occurring without significant subducted water, as our data and vK11's model suggest. Instead, South American slabs likely retain considerably more water past 240 km depth than the model indicates and are more similar to deep hydrous slabs in other colder subduction zones. Indeed, taking this caveat into account, nearly all of the remaining subduction zones with little or no water subducted past 240 km show no seismicity below 240 km. Thus, the data are consistent with a hypothesis that some subducted water is necessary to produce seismicity below 240 km.

Finally, temperature may play an important role in this study. Fig. 4 shows the number of earthquakes per km along trench per year between 240 and 400 km depth from all subduction zones in this analysis, colored by thermal parameter, Φ. Phi, the product of the slab age, the convergence velocity perpendicular to the trench, and sine of the slab dip angle (Syracuse et al., 2010) is a measure of slab temperature at depth, with larger thermal parameters indicating cooler slabs. Here, slabs with Φ < 2500 km are considered hot, 2500 km < Φ < 5000 km are of intermediate temperature, and 5000 km < Φ are considered to be cold (Φ values from Syracuse et al., 2010, shown in Table 1). At 240–400 km, all of the hot slabs are grouped near each other in Fig. 4, the intermediate temperature slabs occupy the intermediate space, and the cold slabs are dispersed across the right side of the figure. This plot emphasizes that the hydration state of a slab depends on temperature. It is therefore challenging to determine whether the earthquakes are caused by dehydration or another factor that depends on temperature.

5. Conclusions

No correlation is found at 75–240 km depth between the number of earthquakes per km along trench per year and the amount of H_2O released by dehydration reactions, despite many authors attributing earthquakes at those depths to dehydration embrittlement. The lack of correlation suggests four possible explanations. First, vK11's dehydration models may be inaccurate because slab input parameters or local geometry variations are not known or taken into account accurately. Second, earthquakes at intermediate depths may not be caused by dehydration. Third, it is possible that intermediate depth earthquakes occur via

dehydration embrittlement, but that other factors such as slab stress control the seismicity rate. Finally, the hydrous products of dehydration reactions may cause intermediate-focus earthquakes, but those events may not occur in exactly the same places as the dehydration reactions.

We find that subduction zones with a higher H_2O flux past 240 km depth have a larger median number of earthquakes at depths of 240–700 km. All slabs subducting a significant amount of water past 240 km depth show some deep seismicity. This suggests that H_2O may enable deep earthquakes in the presence of some other factor that modulates the seismicity rate. We do note with caution that dehydration reactions depend chiefly on temperature, so it is difficult to distinguish the effects of temperature and dehydration when doing comparative studies of subduction zones.

Acknowledgments

We thank Patrick Shore for computer assistance. This work was funded by the National Science Foundation under grants OCE-0752476 and EAR-0842295 and EAR- 0745588.

References

Capitanio, F.A., Faccenna, C., Zlotnink, S., Stegman, D.R., 2011. Subduction dynamics and the origin of Andean orogeny and the Bolivian orocline. Nature 480, 83–86, http://dx.doi.org/10.1038/nature10596.

Chollet, M., Daniel, I., Koga, K.T., Petitgirard, S., Morard, G., 2009. Dehydration kinetics of talc and 10 A phase: Consequences for subduction zone seismicity. Earth Planet. Sci. Lett. 284, 57–64, http://dx.doi.org/10.1016/j.epsl.2009.04.008.

Connolly, J.A.D., 2009. The geodynamic equation of state: What and how. Geochem. Geophys. Geosyst. 10, Q10014, http://dx.doi.org/10.1029/2009GC002540.

Dobson, D.P., Meredith, P.G., Boon, S.A., 2002. Simulation of subduction zone seismicity by dehydration of serpentine. Science 298, 1407–1410, http://dx.doi.org/10.1126/science.1075390.

Estabrook, C.H., 1999. Body wave inversion of the 1970 and 1963 South American large deep-focus earthquakes. J. Geophys. Res. 104, 28751–28767, doe 10.1029/1999JB900244.

Frohlich, C., 2006. Deep Earthquakes. Cambridge University Press, Cambridge, England 23, 101–108, 267–279.

Green, H.W., Burnley, P.C., 1989. A new self-organizing, mechanism for deep-focus earthquakes. Nature 341, 733–737, http://dx.doi.org/10.1038/341733a0.

Green, H.W., Houston, H., 1995. The mechanics of deep earthquakes. Ann. Rev. Earth Planet. Sci. 23, 169–213.

Green, H.W., Chen, W., Brudzinski, M., 2010. Seismic evidence of negligible water carried below 400-km depth in subducting lithosphere. Nature 467, 828–831, http://dx.doi.org/10.1038/nature09401.

Griggs, D., Handin, J., 1960. Observations on fracture and a hypothesis of earthquakes. Geol. Soc.. Amer: Mem. 79, 347–373.

Hacker, B.R., 2008. H_2O Subduction beyond arcs. Geochem., Geophys., Geosyst. 9, Q03001, http://dx.doi.org/10.1029/2007GC001707.

Hacker, B.R., Peacock, S., Abers, G.A., Holloway, S.D., 2003. Subduction factory 2: Are intermediate-depth earthquakes in subducting slabs linked to metamorphic dehydration reactions? J. Geophys. Res. 108 (B1).

Hamburger, M.W., Isacks, B.L., 1987. Deep Earthquakes in the Southwest Pacific: a Tectonic Interpretation. J. Geophys. Res. 92 (B13), 13,841–13,854.

Healy, D., Reddy, S.M., Timms, N.E., Gray, E.M., Brovarone, A.V., 2009. Trench-parallel fast axes of seismic anisotropy due to fluid-filled cracks in subducting slabs. Earth Planet. Sci. Lett. 283, 75–86, http://dx.doi.org/10.1016/j.epsl.2009.03.037.

Hobbs, B.E., Ord, A., 1988. Plastic instabilities: implications for the origin of intermediate and deep focus earthquakes. J. Geophys. Res. 93, 10521–10540.

Holland, T.J.B., Powell, R., 1998. An internally consistent thermodynamic data set for phases of petrological interest. J. Metamorph. Geol. 16, 309–343, http://dx.doi.org/10.1111/j.1525-1314.1998.00140.x.

Houston, H., 2007. Deep Earthquakes. In: Schubert, G. (Ed.), Treatise on Geophysics, Volume 4. Earthquake Seismology, Elsevier, Amsterdam, pp. 321–350.

Hubbert, M.K., Rubey, W.W., 1959. Role of fluid pressure in overthrust faulting. Geol. Soc. Amer: Null. 70, 115–206.

Jung, H., Green, H.W., Dobrzhinetskaya, L.F., 2004. Intermediate-depth erthquake faulting by dehydration embrittlement with negative volume change. Nature 428, 545–549, http://dx.doi.org/10.1038/nature02412.

Kawakatsu, H., 1991. Insignificant isotropic component in the moment tensor of deep earthquakes. Nature 351, 50–53, http://dx.doi.org/10.1038/35100a0.

Kelemen, P.B., Hirth, G., 2007. A periodic shear-heating mechanism for intermediate-depth earthquakes in the mantle. Nature 446, 787–790, http://dx.doi.org/10.1038/nature05717.

Kirby, S.H., 1987. Localized Polymorphic Phase Transformations in High-Pressure Faults and Applications to the Physical Mechanism of Deep Earthquakes. J. Geophys. Res. 92, 13789–13800.

Kirby, S.H., Stein, S., Okal, E.A., Rubie, D., 1996. Deep earthquakes and metastable mantle phase transformations in subducting oceanic lithosphere. Rev. Geophys. Space Phys. 34, 261–306.

Kita, S., Okada, T., Nakajima, J., Matsuzawa, T., Hasegawa, A., 2006. Existence of a seismic belt in the upper plane of the double seismic zone extending in the along-arc direction at depths of 70-100 km beneath NE Japan. Geophys. Res. Lett 33, L24310.

Lee, R.W., Kirby, S.H., 1984. Experimental deformation of topaz crystals: possible embrittlement by intracrystalline water. J. Geophys. Res. 89, 4161–4166, http://dx.doi.org/10.1029/JB089iB06p04161.

Leith, A., Sharpe, J.A., 1936. Deep-focus earthquakes and their geological significance. J. Geol. 44, 877–917.

Mishra, O.P., Zhao, D., 2004. Seismic evidence for dehydration embrittlement of subducting Pacific slab. Geophys. Res. Lett. 31 http://dx.doi.org/10.1029/2004GL019489.

Murrell, S.A.F., Ismail, I.A.H., 1976. The effect of decomposition of hydrous minerals on the mechanical properties of rocks at high pressures and temperatures. Tectonophysics 31, 207–258.

Ogawa, M., 1987. Shear instability in a viscoelastic material as the cause of deep focus earthquakes. J. Geophys. Res. 92, 13,801–13,810.

Okal, E.A., 1996. Radial modes from the great 1994 Bolivian earthquake: no evidence for an isotropic component to the source. Geophys. Res. Lett. 23, 431–434, http://dx.doi.org/10.1029/96GL00375.

Raleigh, C.B., Paterson, M.S., 1965. Experimental deformation of serpentinite and its tectonic implications. J. Geophys. Res. 70, 3965–3985.

Russakoff, D., Ekstrom, G., Tromp, J., 1997. A new analysis of the great 1970 Colombia earthquake and it isotropic component. J. Geophys. Res. 102, 20423–20434, http://dx.doi.org/10.1029/97JB01645.

Schmidt, M.W., Vielzeuf, D., Auzanneau, E., 2004. Melting and dissolution of subducted crust at high pressures: The key role of white mica. Earth Planet. Sci. Lett. 228, 65–84, http://dx.doi.org/10.1016/j.epsl.2004.09.020.

Scholz, C.H., 1989. Mechanics of faulting. Annu. Rev. Earth Planet. Sci. 17, 309–334.

Sdrolias, M., Müller, R.D., 2006. Controls on back-arc basin formation. Geochem. Geophy. Geosys 7 http://dx.doi.org/10.1029/2005GC001090.

Syracuse, E.M., Abers, G.A., 2006. Global compilation of variations in slab depth beneath arc volcanoes and implications. Geochem. Geophys. Geosyst. 7, Q05017, http://dx.doi.org/10.1029/2005GC001045.

Syracuse, E.M., van Keken, P.E., Abers, G.A., 2010. The global range of subduction zone thermal models. Phys. Earth and Planet. Int. 183, 73–90, http://dx.doi.org/10.1016/j.pepi.2020.02.004.

Van Avendonk, H.J.A., Holbrook, W.S., Lizarralde, D., Denyer, P., 2011. Structure of the subducting Cocos plate offshore Nicaragua and Costa Rica. Geochem, Geophys, Geosyst. 12, Q06009, http://dx.doi.org/10.1029/2011GC003592.

Van Keken, P.E., Hacker, B.R., Syracuse, E.M., Abers, G.A., 2011. Subduction Factory 4: Depth-dependent flux of H_2O from subducting slabs worldwide,. J. Geophys. Res. 116 http://dx.doi.org/10.1029/2010JB007922.

Wadati, K., 1928. Shallow and deep earthquakes. Geophy. Mag 1, 161–202.

Yamasaki, T., Seno, T., 2003. Double seismic zone and dehydration embrittlement of the subducting slab. J. Geophys. Res. 108 http://dx.doi.org/10.1029/2002JB001918.

Zhang, J., Green, H.W., Bozhilov, K., Jin, Z., 2004. Faulting induced by precipitation of water at grain boundaries in hot subducting oceanic crust. Nature 428, 633–636, http://dx.doi.org/10.1038/nature02475.